Available online at www.sciencedirect.com
SCIENCE DIRECT®
International Journal of Solids and Structures 42 (2005) 2199–2210
INTERNATIONAL JOURNAL OF SOLIDS and STRUCTURES
www.elsevier.com/locate/ijsolstr

Symmetric and asymmetric deformation transition in the regularly cell-structured materials. Part I: experimental study

Kanyatip Tantikom [a,*], Tatsuhiko Aizawa [b,*], Toshiji Mukai [c]

[a] *Graduate School of Engineering, The University of Tokyo, Tokyo 153-8904, Japan*
[b] *Center for Collaborative Research, The University of Tokyo, Tokyo 153-8904, Japan*
[c] *National Institute for Materials Science, Tsukuba, Ibaraki 305-0047, Japan*

Received 4 June 2004; received in revised form 18 September 2004
Available online 28 October 2004

Abstract

Quasi-static compressive response of regularly cell-structured materials is experimentally studied for various relative density, cell contact length and intercell bonding state. Each cell in this specimen is aligned in a hexagonal closed-pack array. The contact length as well as cell wall thickness of regularly cell-structured materials, plays an important role on the deformation mode transition. The deformation changes itself from symmetric to asymmetric pattern when increasing the contact length to cell-wall thickness ratio. Higher level of collapsing stress is observed in symmetric deformation due to the nearly uniform stress transfer during compression. Work hardening behavior is promoted with increasing the relative density or decreasing the contact length. Asymmetric deformation is associated with a nearly constant collapsing stress. The plateau collapsing stress state is caused by the localized deformation of cell-row in a narrow band of specimen. Liquid epoxy resin between cell walls also influences on the deformation mode of cell-structured materials. In the present study, the experimental observation is presented first (Part 1), followed by the theoretical analysis and comparison between experimental and analytical results in (Part 2).

Keywords: Cell-structured materials; Metal honeycomb; Lightweight structure; Mechanical property; Cellular solids

* Corresponding authors. Address: Metallurgy Department, The University of Tokyo, Meguro ku Komaba, Tokyo, Japan. Tel.: +819061 848349; fax: +81 354 525116 (K. Tantikom), tel.: +84 354 525086; fax: +84 354 525116 (T. Aizawa).
E-mail addresses: kanyatip@odin.hpm.rcast.u-tokyo.ac.jp (K. Tantikom), aizawa@odin.hpm.rcast.u-tokyo.ac.jp (T. Aizawa).

0020-7683/$ - see front matter © 2004 Elsevier Ltd. All rights reserved.
doi:10.1016/j.ijsolstr.2004.09.028

1. Introduction

There has been an increasing interest for lightweight constructions and designs. Various sandwich panels were preferable for light and stiff structures, where a high stiffness is added in order to prevent these parts from vibrating or torsional deformation. Honeycomb structure was invented to improve the specific strength of materials especially for out-of-plane compression (Gibson and Ashby, 1997). A further important application field for cellular structures is energy absorption. Using suitable structural design, it is possible to induce a controlled, deformation pattern in the crashed zone with maximum energy consumption (Mukai et al., 1999; Kanahashi et al., 2002). The cellular structure gives rise to a unique combination of properties, which is exploited in engineering design: e.g., low density, high-energy absorption capacity, and low thermal conductivity (Gibson, 2003). These types of cellular materials are characterized by high strength-to-weight ratio (Hayes et al., 2002; Clark et al., 2002) and/or large compressive loading capacity (Yamada et al., 2000; Kanahashi et al., 2001).

Recently, much attractiveness is found in cellular solids for multifunctional applications. High loading capacity is required together with other functionalities: e.g., ultra-light structure, oxide catalysts, compact cooling, and energy absorption or vibration control. Metallic honeycomb structures feature important properties such as light weight and comparable strength with respect to monolithic geometries. Some of these applications include load bearing structures, thermal management, sound absorption and other areas where their beneficial properties are needed to coincide with low-density structures (Nadler et al., 2002). These new opportunities are emerging for two reasons. First, the novel manufacturing approaches have beneficially affected performance and cost. Secondly, basic understanding about mechanical, thermal and acoustic properties have been developed in the higher level in conjunction with the associated design strategies. These provide an integrated pathway between manufacturing and design (Evans et al., 1998).

Optimal morphological design of cellular materials is one of the main issues in structural material design. The size, shape and topology of cell walls have a significant impact on the mechanical and thermal properties (Aizawa et al., 2002; Tantikom et al., 2003; Hayes et al., 2004). In addition, precise understanding of material response is also necessary to describe the loading capacity and to make topological optimization of two-dimensional cell-structured materials (Shim and Stronge, 1986; Tantikom et al., 2004).

In the present study, a hexagonal close-packed array of copper tubes is selected as a representative of structural pattern since this material can be mechanically joined at relatively low temperature without any bonding medium. Uniaxial in-plane compression of nearly perfect cell-structured specimens is experimentally observed. In order to achieve the mechanical understanding in deformation transition of cell-structured materials, various parameters are varied and examined such as relative density, contact length, and adhesive bonding of regularly cell-structured materials. Elasto-plastic deformation behavior and stress–strain responses of the two-dimensional regularly cell-structured materials are investigated under quasi-static compression.

2. Experimental procedure

In order to understand the mechanical response of regularly cell-structured materials, a unit model of metallic tube-array was fabricated by mechanical joining. Pure copper tubes (Nakajima Precision Tube IND. Co., Ltd.) were selected for various aspect ratio of radius to thickness, to fabricate the regular-hexagonally packed array of tubes. Tube geometries are listed in Table 1. These tubes were cut into specimens with the length of 5 mm. They were surface treated by ultrasonic cleaning in acetone for 300 s, dipped in 3% HCl for 60 s and 10% H_2SO_4 solution at 333 K for 30 s, respectively.

Pure copper tubes with the specified number of rows and columns were assembled into a hexagonal close-packed arrangement in an alumina box. Copper tubes were jointed in a vacuum furnace at 1023 K.

Table 1
Dimension of tubes used in the experiment

Material	Outer radius (R, μm)	Thickness (t, μm)	R/t
Pure Cu	400	80	5.0
Pure Cu	400	50	8.0

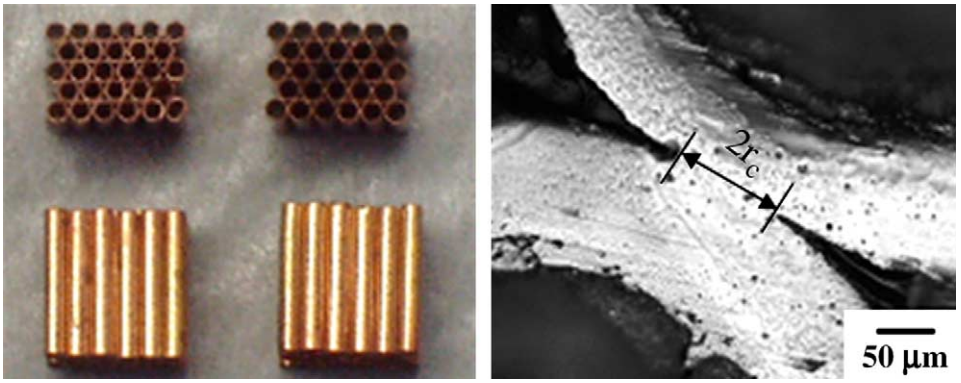

Fig. 1. Regularly copper cell-structured specimens and contact area between two cell walls.

The box was held for 10.8 ks to homogenize the microstructure of bonding area. Difference in thermal expansion coefficient between metallic tubes and the alumina die-box caused the compressive stress during heat treatment. Through this bonding, each tube was tightly connected with each other to form copper cell-structured assemblies. Fig. 1 depicts the regularly cell-structured array and the contact area between two cell walls.

In-plane compression tests were carried out by the universal testing machine (Autograph Shimadzu) with the loading rate of 0.24 mm/min. The compression tests were also done by the Shimadzu-Servopulser testing machine connected with the JEOL (JSM-5410LV) scanning electron microscope to observe the deformation behavior of cell-structured specimens, as shown in Fig. 2.

The in-plane nominal compressive stress (σ_c) is defined by dividing the load (P) by the original cross-sectional area of the specimen (A_0):

$$\sigma_c = P/A_0. \tag{1}$$

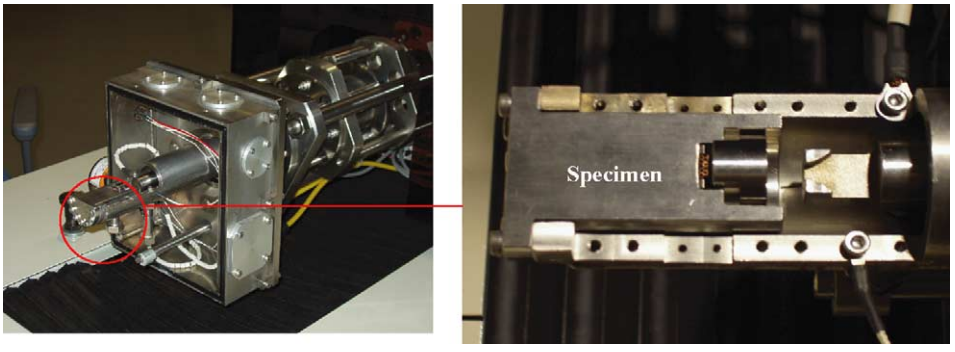

Fig. 2. Specimen fixed in SEM-Servopulser before compressive testing.

The specific compressive stress is defined by σ_c/ρ_R. The nominal compressive strain (ε_c) is calculated by dividing the displacement of upper punch (δ) by the original height of specimen (h_0):

$$\varepsilon_c = \delta/h_0. \tag{2}$$

3. Verification of regularly cell-structured specimen

In-plane compression was conducted to consider the effect of number of rows on the deformation behavior. The assemblies have the same radius of 400 μm, the thickness of 80 μm and the relative density of 0.29. The loading condition overwhelms the intrinsic stress–strain response of the cell-structured materials when the number of rows is small in the assembly. Fig. 3 compares the nominal stress–strain relations among three-row, five-row and seven-row aligned specimens. The elastic region is vaguely observed in the three-row assembly while the linear elastic region is present in the stress–strain relations for the five-row and seven-row assemblies. The cell-structured specimen has a positive slope with $d\sigma_c/d\varepsilon_c > 0$ in the collapsing region. In addition, the densification starts at the lower strain in the three-row specimen. These dissimilar features are caused by the different number of cells which are adjacent to the punches. Deformation of adjacent cells to the punches is constrained by the loading motion of punches. The top and bottom end rows have higher stiffness than other inner cells. Fig. 4 compares the deformed geometry of specimens at the compressive strain of 20%. Uniform symmetric deformation is observed in all of the specimens. Since little

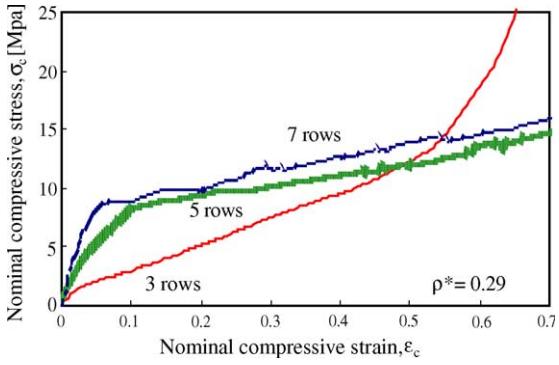

Fig. 3. In-plane compressive stress–strain curves of pure copper assemblies with different number of rows.

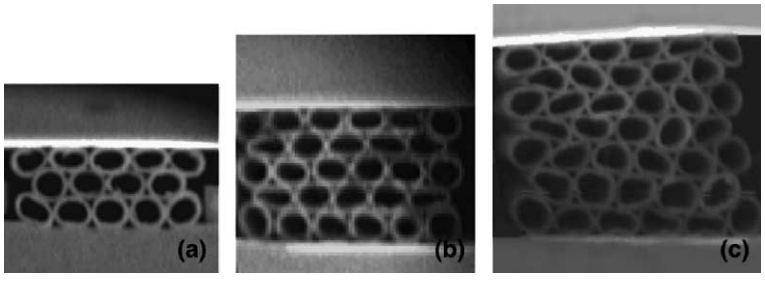

Fig. 4. Deformed specimens at 20% compressive strain: (a) three-row specimen, (b) five-row specimen, and (c) seven-row specimen.

significant difference was seen between five- and seven-row specimens, five-row specimen was employed as a representative model to demonstrate the mechanical response of regularly cell-structured materials in this study.

As first discussed on the optimum design of unit cell structure (Tantikom et al., 2004), the deformation mode changes itself with loading condition in the regularly cell-structured assembly. In particular, the mode change in the collapsing stage affects on the absorption energy in crushing of cell-structured materials. Fig. 5 compares two types of deformation sequence for the regularly copper cell-structured specimens with the same relative density. As shown in Fig. 5(a), the cell-structured specimen deforms symmetrically without topological change in the hexagonal array packing. Each constituent cell in the assembly except for the top and bottom ends, plastically collapses along the vertical axis. This symmetric deformation is essentially uniform throughout the specimen.

The regularly cell-structured materials also deform in the asymmetric mode. As shown in Fig. 5(b), after initial symmetric deformation up to $\varepsilon_c = 10\%$, the shear type localization occurs in the narrow zone. In this case, cells in the second row from the bottom begin to make shear-deformation while the remote cells from this zone, near the top of specimen, remain to make symmetric deformation. This local collapsing deformation progresses successively in each two neighboring row until it is arrested by the cell walls in contact. This shear-type deformation mode is commonly observed in the circular cell-structured materials (Shim and Stronge, 1986; Poirier et al., 1992; Papka and Kyriakides, 1998; Chung and Waas, 2002).

As reported in the above literature, no symmetric deformation is often observed in the cell-structured materials. This might be because of the irregularity of cell alignment and cell-wall thickness. In other words, it is strongly dependent on the initial geometric and material conditions, whether the uniform symmetric deformation is selected in compression as more stable configuration than the shear-type asymmetric deformation.

A cell-element located at the center of specimen, is employed as a representative local unit. Fig. 6 plots its true strain ε^* of the representative cell versus the global compressive strain ε_c. For symmetric deformation, linear proportionality between ε^* and ε_c during compressive loading, assures that each cell-element deforms with nearly the same strain as nominal one. For asymmetric deformation, ε^* increases abruptly when $\varepsilon_c > 0.15$. Since this cell element locally collapses, it has little loading capacity for $\varepsilon_c > 0.15$. The local collapsing behavior is accompanied with the significantly large spin rotation.

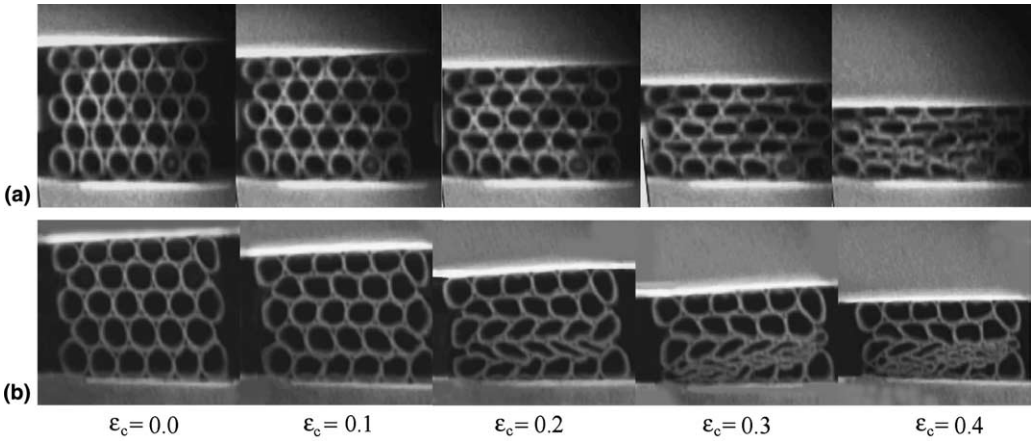

Fig. 5. Deformation sequences of copper cell-structured assemblies: (a) symmetric deformation, and (b) a symmetric deformation.

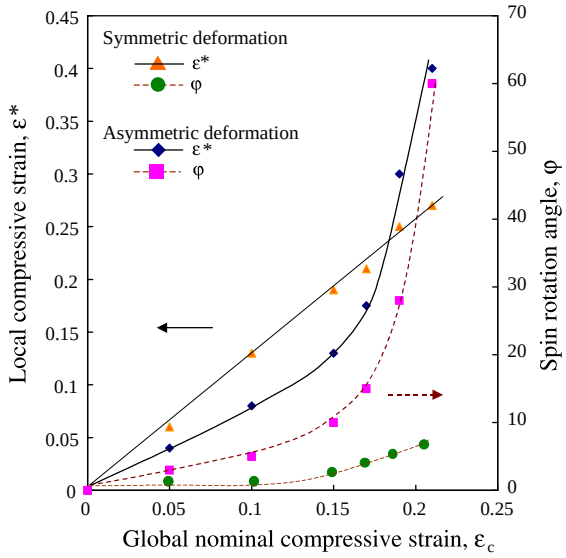

Fig. 6. Compressive straining behaviors of representative cells for both collapsing behaviors.

4. Parameter survey

Effects of the relative density, the contact length and the adhesive bonding on the deformation mode are experimentally investigated to describe the parameter sensitivity in the regularly cell-structured materials.

4.1. Relative density

In order to study the effect of relative density on the compressive behavior, copper tube wall thickness was varied from 50 to 80 μm, with the diameter of 800 μm and the average contact length (r_c) of 25 μm. The relative densities (ρ_R) of these specimens were 0.19 and 0.29 respectively. Fig. 7 shows the nominal stress–strain curves for two specimens. No difference is seen at the early stage of elastic region. When $\rho_R = 0.29$, the work hardening takes place in the collapsing stage, while the stress becomes nearly constant

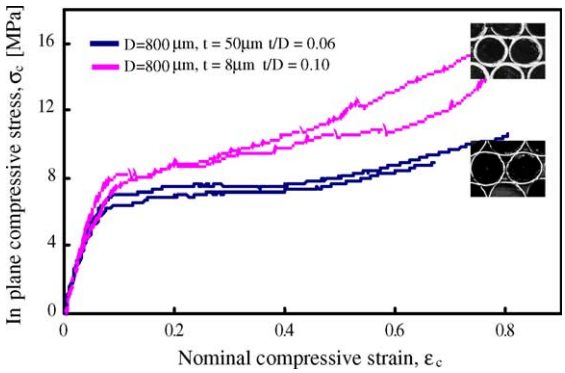

Fig. 7. In-plane compressive stress–strain curves of copper assemblies with different relative density.

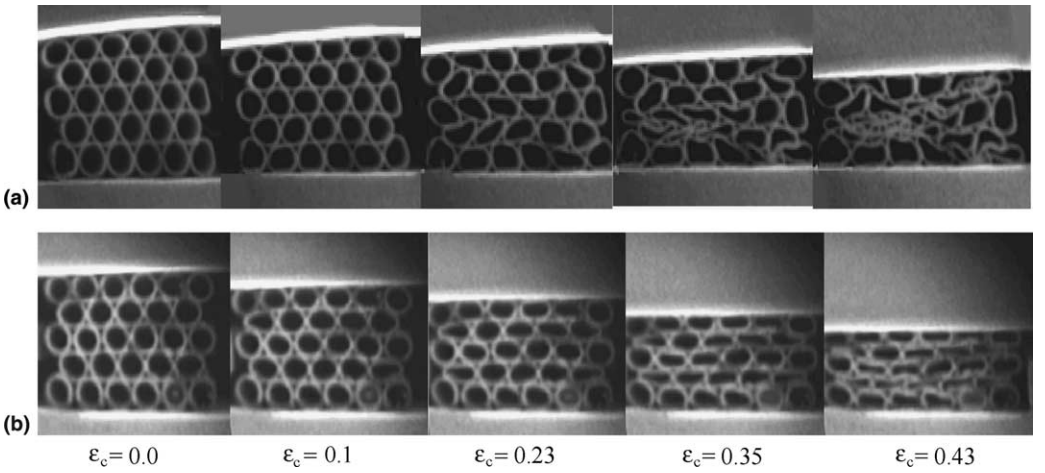

Fig. 8. Deformation sequences of regularly cell-structured assemblies: (a) $\rho_R \approx 0.19$, and (b) $\rho_R \approx 0.29$.

($d\sigma_c/d\varepsilon_c \approx 0$) when $\rho_R = 0.19$. Sequence of deformed geometry of specimens taken by SEM-Servopulser for these two specimens was shown in Fig. 8. Initially, both assemblies deform in the symmetric mode up to 10% in compressive strain. For large compressive strain, localization initiates in the low relative density specimen, while the symmetric deformation is preserved in the high relative density assembly. This localized collapsing results in the nearly uniform plateau stress in the lower relative density specimen.

4.2. Contact length

In order to study the effect of contact geometry on the mechanical response of regularly cell-structured materials, the contact length between neighboring cell walls was varied in the preparation of specimens. The average contact length (r_c) of cell-structured specimens was controlled to be 25–50 μm with the radius of 400 μm, the thickness of 80 μm and the relative density of 0.29. Fig. 9 shows the in-plane compressive stress–strain relationship of two cell-structured specimens with the same size and relative density but different contact lengths: (a) larger contact length specimen with $r_c/t = 0.6$, and (b) smaller contact length

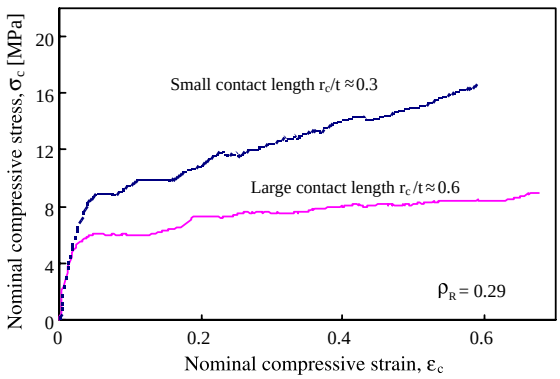

Fig. 9. In-plane compressive stress–strain curves of pure copper assemblies with different contact lengths.

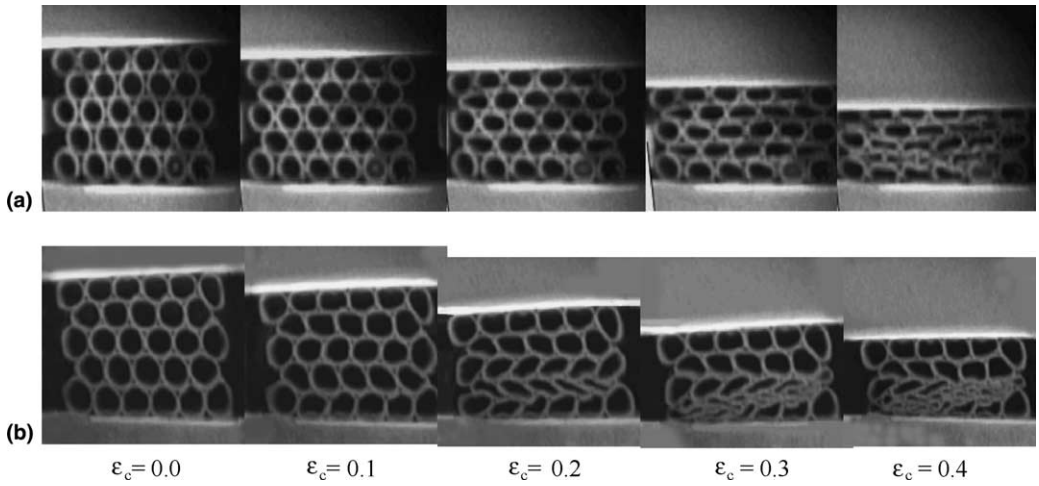

Fig. 10. Deformation sequences of copper cell-structured assemblies: (a) small contact length, and (b) large contact length.

specimen with $r_c/t = 0.3$. In the former, the initial yielding stress $\sigma_{initial}$ becomes 6.1 MPa and the average plateau stress σ_{ave}, 7.3 MPa. Since σ_{ave} is nearly equal to $\sigma_{initial}$, little work hardening takes place in the collapsing deformation stage. In the latter, $\sigma_{initial} = 9.0$ MPa and $\sigma_{ave} = 12.9$ MPa; $\sigma_{ave} > \sigma_{initial}$. Significant work hardening takes place together with collapsing. This difference just corresponds to the in-plane compressive deformation mode in Fig. 10. In the former, the symmetric deformation remains in the whole stage of collapsing up to $\varepsilon_c = 0.4$. In the latter, the initial symmetric deformation takes mode-transition to the asymmetric deformation with localization. This proves that the local cell geometry plays an important role on the in-plane compression response of the regularly cell-structured materials.

4.3. Adhesive bonding

Liquid epoxy resin D.E.R 331J (Dow Chemical Company) was selected as a bonding medium between cell walls of copper cell-structured specimen. Table 2 is listed typical properties of D.E.R 331J epoxy resin. Fig. 11 shows microstructure of mechanical joining cell-structured specimen dipped in resin with the diameter of 800 μm, the thickness of 80 μm, the relative density of 0.29, and the average contact length of 25 μm. Copper cell-structured specimen with resin, collapses by uniform symmetric deformation, as shown in Fig. 12. Its specific stress–strain relationship was compared to mechanically joined cell-structured specimen in Fig. 13. The dipped resin specimen has higher yielding stress and plastic modulus than the mechanically joined specimen. Work-hardening is clearly seen in the collapsed region. This assures that local stress transfer across the cell walls should influence on the stress level and deformation mode transition.

Table 2
Properties of D.E.R. 331J liquid epoxy resin

Viscosity at 25 °C (mPa s)	16,000–25,000
Density at 25 °C (g/ml)	1.14
Flash Point, (°C)	252
Shelf life (months)	24

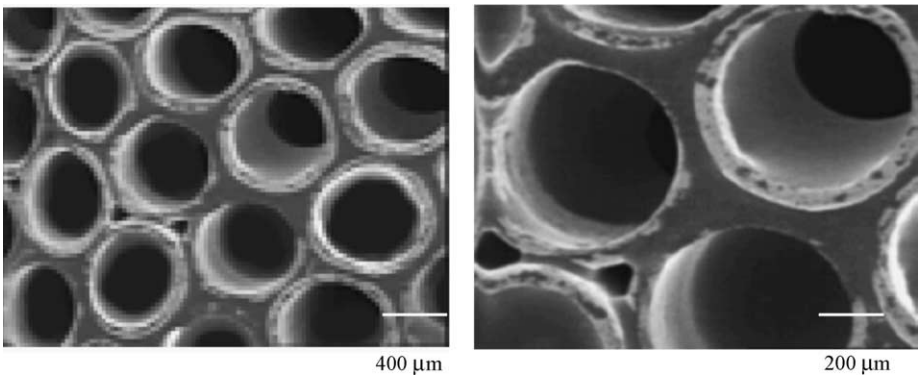

Fig. 11. SEM images of copper cell-structured material after dipped in liquid epoxy resin.

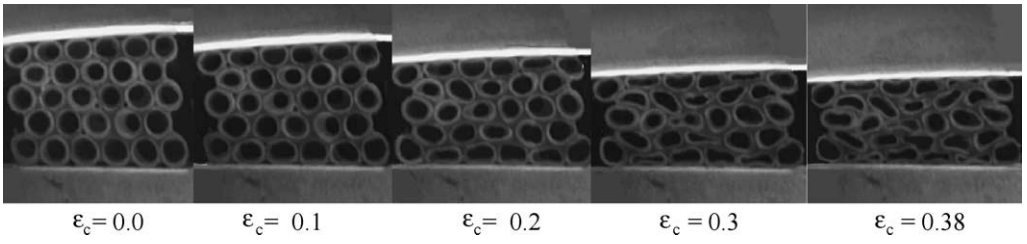

Fig. 12. Deformation sequence of pure copper dipped resin assembly.

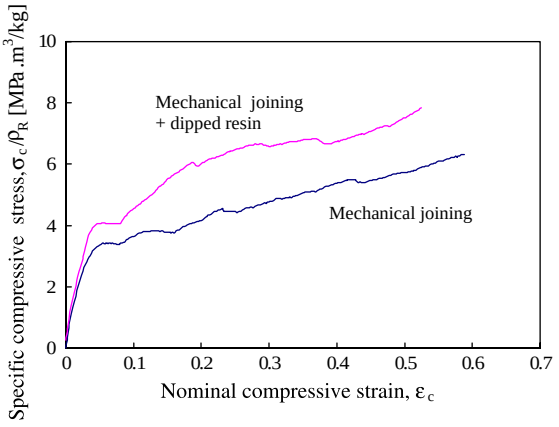

Fig. 13. Compressive stress–strain curves of pure copper assemblies with and without adhesive bonding.

5. Discussion

In the experimental observation of the collapsing deformation for the regularly cell-structured specimen, two different deformation modes are present: symmetric and asymmetric collapsing modes. The former is characterized by uniform compression without localized shear deformation. Under this situation, initial yielding behavior of cell-structured materials is followed by significant work hardening. This mechanical

response in compression was never reported in literature. In the latter, the deformation mode changes itself to the asymmetric collapsing mode with localization just after the initial yielding.

According to the reference on the plasticity of bulk or porous solids in compression (Hill, 1999), the whole medium plastically reduces in height without shear localization. Corresponding to this general feature, all the cells in the cell-structured materials uniformly collapses at the same time during the symmetric deformation. Since each cell sustains the applied compressive load from the upper punch, higher loading capacity is experienced with work hardening. Hence, the nominal stress–strain relationship in the symmetric deformation approaches to the stress–strain relation of bulk dense materials with increasing the relative density. That is, the initial yield stress (σ_y) and the plastic modulus (K_p) are thought to converge to the material yield stress (σ_y^o) and the material plastic modulus (K_p^o) when ρ_R approaches to unity.

The above symmetric deformation often branches to more stable equilibrium path in compression. As had been discussed in the bifurcation theory (Chajes, 1974), the symmetrically deforming solid branches or snaps-through above the critical compressive load. In the case of elasto-plastic response of the regularly cell-structured materials, the branching point in the symmetric-to-asymmetric mode transition, might be stable so that the mixed deformation mode could be seen at this point.

In the asymmetric deformation mode, shear-localization initiates from the weakest cell and spreads from one collapsing zone to its neighboring cells. This successive propagation of cell-collapsing continues until the onset of densification. Different from the stable branching from symmetric to asymmetric modes, this continuous localization from the weakest cell becomes unstable so that the asymmetric deformation advances without the appearance of work-hardening. Namely, the initial yielding stress becomes lower than that in the symmetric deformation and K_p is nearly zero, or, nearly constant plateau stress is experienced in the collapsing stage. In other words, the appearance of constant plateau stress in the stress–strain relationship, is a proof that successive shear-localization advances from the weakest cell to the rest of materials until the onset of densification.

As had been indicated by textbook (Gibson and Ashby, 1997), the relative density or the cell-wall thickness plays an important role on the elasto-plastic deformation of cell-structured materials. As mentioned before, the uniform symmetric deformation mode is selected as an equilibrium path with increasing the relative density. When the relative density decreases or the cell-wall thickness reduces, the sensitivity to local weakening is enhanced so that the mode transition takes place at lower nominal strain. From experiments, $\rho_R^* \approx 0.3$ might be a critical relative density. When ρ_R is lower than ρ_R^*, the local sensitivity is enhanced by other geometric parameters.

The contact length between adjacent cell walls has a significant influence on this mode transition. Even if the cell-materials have the same relative density, increase of contact length leads to enhancement of mode transition. That is, asymmetric deformation is selected after initial yielding when the cell-structured materials have larger contact length or contact area. As partially discussed in the reference (Tantikom et al., 2004), this influence on the mode transition is explained by local stress transfer. When r_c is small, the stress uniformly transfers though the contact wall thickness even in the collapsing stage. There is little or no local network in stress transfer. With increasing r_c, the local network for stress transfer forms during the collapsing stage, so that plastic deformation concentrates on this network. The rest of materials recover from the elasto-plastic to elastic states. This plastic localization with unloading behavior in the rest, stimulates the asymmetric deformation.

In the present regular cell-alignment, ρ_R increases with t once the cell diameter is fixed. With increasing ρ_R or t, the symmetric mode is easily selected. On the other hand, the asymmetric mode is selected with increasing the contact length. Hence, r_c/t might be a good indicator to describe the mode transition.

In order to demonstrate the role of local stress transfer on the mode transition, a deformable, viscous medium is fixed among the connected cells. At the presence of deformable buffer, cell-structured specimen becomes denser and more isotropic. Hence, the compressive deformation of regularly cell-structured materials advances in more uniform and stable in collapsing. In addition, the viscous medium between adjacent

cell walls helps supporting the compressive loading. The higher specific collapsing stress and significant strain hardening in post-yielding region can be attained in the dipped resin specimen. Thus, the local stress transfer across the cell walls significantly influences on the collapsing stress level and deformation mode transition of regularly cell-structured materials.

6. Conclusion

The regularly cell-structured material is fabricated by the mechanical joining method. Nearly perfect cell-structured specimens are used to investigate the compressive stress–strain relation and their deformation mode of regularly cell-structured materials. The specimen at least with the five-row close-packed array has an intrinsic stress–strain relationship to the cell-alignment without the effect of number of cells. The relative density or cell-wall thickness have an influence on the collapsing stress level and the sensitivity to localized deformation. The contact length between the adjacent cell walls plays an important role on the deformation mode transition. Symmetric deformation advances in the specimen with small contact length due to the uniform stress transfer across the contact area. Increasing the contact length, the asymmetric deformation is promoted because the plastic deformation concentrates in a local network. This plastic localization is accompanied with severe distortion in the weakest cell. The subsequent collapsing deformation among the adjacent cells and adjacent rows, results in the nearly constant plateau stress in the stress–strain relation. Higher specific collapsing stress is attained for the dipped resin specimen. The presence of deformable buffer among the cell walls promotes uniform symmetric deformation. Therefore, the mechanical design of cell-structured materials has to consider the local cell geometry, the local stress transfer as well as the deformation mode change in order to improve the loading capacity in compression.

Acknowledgement

Authors would like to express their gratitude to Dr. S. Yamamoto for his experimental help. This study is financially supported in part by the Grand-in-Aid from MEXT for the project on the barrier-free processing and the environmentally benign manufacturing.

References

Aizawa, T., Kanahashi, H., Tantikom, K., 2002. J. Jpn. Foun. Eng. Soc. 74, 805–811.
Chajes, A., 1974. Principles of Structural Stability Theory. Prentice-Hall, New Jersey.
Chung, J., Waas, M.A., 2002. AIAA J. 40 (5), 966–973.
Clark, J.L., Cochran, K.J., Sanders, T.H., Lee, K.J., 2002. Processing and properties of lightweight cellular metals and structures. In: Proceedings of the 2002 TMS Annual Meeting in Seattle, Washington, pp. 137–146.
Evans, A.G., Hutchinson, J.W., Ashby, M.F., 1998. Progr. Mater. Sci. 43 (3), 171–221.
Gibson, L.J., Ashby, M.F., 1997. Cellular Solids Structure and Properties, second ed. Cambridge University Press, Cambridge, MA.
Gibson, L.J., 2003. Research Topics and Projects for Lorna J Gibson. Available from: <http://www-me.mit.edu/people/research/ljgibson.htm>.
Hayes, A.M., McDowell, D.L., Cochran Jr., K.J., 2002. Processing and properties of lightweight cellular metals and structures. In: Proceedings of the 2002 TMS Annual Meeting in Seattle, Washington, pp. 223–232.
Hayes, A.M., Wang, A., Dempsey, M.B., McDowel, L.D., 2004. Mech. Mater. 36, 691–713.
Hill, R., 1999. The Mathematical Theory of Plasticity. Oxford University Press, Oxford.
Kanahashi, H., Mukai, T., Yamada, Y., Shimojima, K., Mabuchi, M., Aizawa, T., Higashi, K., 2001. Mater. Trans. JIM 42, 2087–2092.
Kanahashi, H., Mukai, T., Nieh, T.G., Aizawa, T., Higashi, K., 2002. Mater. Trans. JIM 43, 2548–2553.

Mukai, T., Kanahashi, H., Miyoshi, T., Mabuchi, M., Nieh, T.G., Higashi, K., 1999. Scri. Mater. 40 (8), 921–927.
Nadler, J.H., Sander, T.H., Cochran, J.K., 2002. Processing and properties of lightweight cellular metals and structures. In: Proceedings of the 2002 TMS Annual Meeting in Seattle, Washington, pp. 147–155.
Papka, D.S., Kyriakides, S., 1998. Int. J. Solids Struct. 35, 239–267.
Poirier, C., Ammi, M., Bideau, D., Troadeem, J.P., 1992. Phy. Rev. Lett. 68 (2), 216–219.
Shim, V.P.W., Stronge, W.J., 1986. Int. J. Mech. Sci. 28, 709–728.
Tantikom, K., Kanahashi, H., Yamamoto, S., Aizawa, T., 2003. Mater. Trans. JIM 44, 1290–1294.
Tantikom, K., Suwa, Y., Aizawa, T., 2004. Mater. Trans. JIM 45, 509–515.
Yamada, Y., Shimojima, K., Sakaguchi, Y., Mabuchi, M., Nakamura, M., Asahina, T., Mukai, T., Kanahashi, H., Higashi, K., 2000. Mater. Sci. Eng. A 280, 225–228.